

## Photocatalytic and antibacterial activity of Fe-doped TiO<sub>2</sub> nanoparticles prepared by nonhydrolytic sol-gel method

A. M. Stoyanova<sup>1\*</sup>, H. Y. Hitkova<sup>1</sup>, N. K. Ivanova<sup>1</sup>, A. D. Bachvarova-Nedelcheva<sup>2</sup>,  
R. S. Iordanova<sup>2</sup>, M. P. Sredkova<sup>1</sup>

<sup>1</sup> Medical University-Pleven, 5800 Pleven, Bulgaria

<sup>2</sup> Institute of General and Inorganic Chemistry, Bulgarian Academy of Sciences,  
1113 Sofia, Bulgaria

Received February, 2013; Revised May, 2013

In the present work we report synthesis of pure and iron doped TiO<sub>2</sub> by nonhydrolytic sol-gel method using titanium tetrachloride, benzyl alcohol and iron(III) nitrate.

The structure of the resulting particles was characterized by XRD, IR and UV-Vis spectroscopy. The average particles size of Fe-doped TiO<sub>2</sub> was 12–15 nm.

The photocatalytic activity of the as-prepared TiO<sub>2</sub> powders was tested by photodegradation of the organic dye Reactive Black 5 under UV and visible irradiation in an aqueous suspension.

Antibacterial action of pure and Fe-modified titanium dioxide samples was tested using *Escherichia coli* ATCC 25922. The bacterial growth was examined in the presence of a synthesized preparations – in dark and with UV light. The photodisinfection activity was assessed by plotting of survival curves and calculation of removal efficiency. In order to estimate the post-irradiation effect, the behavior of the bacterial suspension in presence of each photocatalyst after 24 h dark period was tested.

The optimal iron content was found to be 0.5 mol% for the photocatalytic decomposition of Reactive Black 5 dye under ultra violet (UV) and visible (Vis) irradiation, and also for antibacterial activity in the presence of UV light. At higher iron contents (1–2 mol%) the photocatalytic performance under both UV and Vis irradiation was worse relative to the undoped TiO<sub>2</sub>.

**Key words:** Fe-doped titanium dioxide, sol-gel, photocatalytic, antibacterial activity.

### INTRODUCTION

Titanium dioxide is a wide-band-gap semiconductor and a well-known photocatalytic material. Nanosized titanium dioxide is used in a variety of applications, such as fine ceramics, cosmetics, gas sensors, inorganic membranes, electronic devices and solar cells [1, 2]. Other photochemical and photophysical applications include photolysis of water and light-induced superhydrophobicity [2]. Because of its favorable physico-chemical properties it is now under intensive investigations for practical application to environmental and antimicrobial purification [2–4]. Many organic compounds can be decomposed in aqueous solution in the presence of TiO<sub>2</sub> powders or coatings illuminated with near UV or sunlight [5–7].

Most investigations on semiconductor catalysis focus on anatase type TiO<sub>2</sub>, because of its high photocatalytic activity under UV irradiation ( $\lambda \geq 388$  nm) [8–10]. Photocatalytic reactions occur on the surface of TiO<sub>2</sub> particles. When TiO<sub>2</sub> is irradiated by UV rays, pairs of positively charged holes are created in the valency band and electrons in the conductivity band. The holes react with water molecules or with the hydroxyl ions and as a result hydroxyl radicals are formed, which are strong oxidants of the organic molecules [2]. Hydroxyl radicals and other photo-generated reactive oxygen species can cause oxidative attack of the bacterial cell membrane and some internal cellular components that finally leads to cell death [11, 12].

However, there are still problems needed to be solved concerning its application in photocatalysis. Its shortcomings include a large band gap energy (3.2 eV) which causes most of the solar spectrum unutilized. In a number of cases, the photocatalytic reactions on TiO<sub>2</sub> nanoparticles can usually be in-

\* To whom all correspondence should be sent:  
E-mail: astoyan@abv.bg

duced only by ultraviolet light, which limits the application of TiO<sub>2</sub> as a photocatalyst with visible light [2, 13]. In addition, the holes may recombine rapidly with conduction band electrons, thus decreasing the photocatalytic oxidation efficiency. Therefore, prolongation of the holes lifetime is favourable for the photocatalytic efficiency. In order to accomplish solar-driven photocatalysis and at the same time retard possible electron-hole recombination, doping of TiO<sub>2</sub> with various transition metals is one of the most successful strategies. Multivalent metal ions act as electron scavengers at the surface of the titanium dioxide, thus preventing electron-hole recombination and improving the oxidation performance [14, 15].

Among various metal ions, doping with iron(III) has been widely investigated because of its unique electronic structure and its size that closely match those of titanium(IV). The favorable electronic states of iron ions in titania contribute to formation of efficient trapping sites for electrons and holes [16, 17]. Enhanced photocatalytic activity was reported for iron-doped TiO<sub>2</sub> under UV and also for visible light irradiation in several publications [16–20]. On the contrary, some authors observed no or even negative effect of iron on the photocatalytic performance [21–24].

The effect of metal ion doping strongly depends on many factors such as synthetic procedure, doping method and the dopant concentration [14, 16]. Iron-doped titania samples have been prepared by various methods, including hydrothermal, controlled hydrolysis, co-precipitation, impregnation, solvothermal, etc. [20]. Among the most popular synthetic methods is sol-gel technology induced by traces of water. However, in most cases the reaction rates in aqueous sol-gel chemistry are very fast, especially with transition metal precursors, making it uneasy to control the processes. A simple way to circumvent this problem is applying of so called nonaqueous or nonhydrolytic procedures – syntheses performed in organic solvents under exclusion of water [25, 26]. The slower reaction rate of nonhydrolytic processes allow for better control over particle size and crystallinity [27].

In view of increasing the photocatalytic activity of TiO<sub>2</sub>, we prepared pure and iron doped TiO<sub>2</sub> by nonhydrolytic sol-gel method and further evaluated their photocatalytic and antibacterial activity.

## EXPERIMENTAL

### Materials

Titanium(IV) chloride (purity ≥99.0%) was purchased from Fluka, benzyl alcohol (≥99.5%)

from Merck, iron(III) nitrate, Reactive Black 5 dye (C<sub>26</sub>H<sub>21</sub>N<sub>5</sub>Na<sub>4</sub>O<sub>19</sub>S<sub>6</sub>, dye content, 55%), absolute ethanol and diethyl ether were supplied by Sigma-Aldrich. All the chemicals were used without further purification.

### Preparation and characterization of titania catalysts

The synthesis of pure and Fe-doped titanium oxide nanoparticles was carried out following the nonhydrolytic procedure described by Niederberger et al. [27]. For the synthesis of undoped TiO<sub>2</sub> titanium tetrachloride was slowly added to a beaker containing benzyl alcohol under vigorous stirring and the resulting sols were heated at 150 °C for 1 h, at continued stirring [28]. For the preparation of Fe-modified TiO<sub>2</sub>, initially, proper amount of iron(III) nitrate was dissolved in ethanol and fed to benzyl alcohol according to Figure 1. The reaction mixtures were left for aging at room temperature for 10–14 days. The resulting white thick suspensions were centrifuged at 4500 rpm for 15 min and the supernatant was discarded by decantation. The precipitates were then washed two times with absolute ethanol and three times with diethyl ether. After every washing

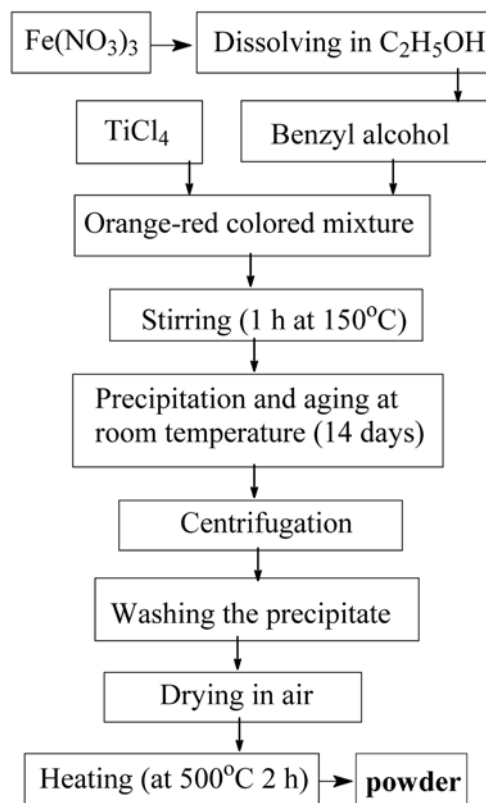


Fig. 1. Scheme of nonhydrolytic synthesis of Fe-doped TiO<sub>2</sub>

step, the solvent was separated by centrifugation. The collected material was dried in air overnight and then ground into a fine powder. The obtained powders were calcinated at 500 °C for 2 hours. The as-prepared samples are denoted as TiO<sub>2</sub> for pure and xFe/TiO<sub>2</sub> for doped titania, where x represents the Fe/Ti mol ratio. In this way three modified TiO<sub>2</sub> samples were obtained: 0.5Fe/TiO<sub>2</sub>, 1Fe/TiO<sub>2</sub>, and 2Fe/TiO<sub>2</sub>.

The structure and morphology of the resulting particles were characterized by X-ray diffraction (XRD, Bruker D8 Advance X-ray apparatus), infrared (IR, using the KBr pellets method (Nicolet-320, FTIR spectrometer with a resolution of ±1 cm<sup>-1</sup>, by collecting 64 scans in the range 4000–400 cm<sup>-1</sup>) and UV-Vis spectroscopy (Spectrophotometer Evolution 300).

#### Photocatalytic activity experiments

The photocatalytic activities of the synthesized powders were evaluated by degradation of a model aqueous solution of the azo dye Reactive Black 5 (RB5) under UV-Vis illumination. The molecular structure of this commercially used dye is given in Figure 2.

The initial concentration of RB5 aqueous solution was 20 mg/l. Titanium sample (100 mg) was added to 150 ml dye solution to form suspension. After sonicated for 10 min, the suspension was magnetically stirred in dark for 30 min to ensure the establishment of an adsorption-desorption equilibrium. The UV-irradiation source was a black light blue lamp (Sylvania BLB 50 Hz 8W T5) with the major fraction of irradiation occurring at 365 nm. The lamp was fixed 10 cm above the solution surface. The intensity of UV-light reaching the surface of the suspension was measured with a numeric Luxmeter (LM 37, Dostmann electronic). The mean value of the radiation power impinging on the reacting suspension was estimated to be 150 Lx.

The visible light source was a 500W halogen lamp (Sylvania) fixed at 40 cm above the treated solution. The mean value of the radiation power reaching on the suspension was estimated to be 14000 Lx.

All photocatalytic tests were performed at constant stirring rate (450 rpm) and room temperature

of 25 °C. At regular time intervals of illumination, aliquot samples of the mixture (3 mL) were collected and centrifuged in order to remove the solid particles. The absorbances of clear aliquots were measured by a Jenway 6505 UV-Vis spectrophotometer at 597 nm, the maximum absorption wavelength of RB5.

#### Antibacterial activity experiments

##### Bacterial strain and preparation of bacterial suspension

*Escherichia coli* ATCC 25922 was used as a model microorganism. To prepare bacterial suspension, one colony from a fresh culture of the tested strain was introduced into Tryptic Soy Broth (Difco) and then grown under aerobic conditions at 37 °C. After 15 hours incubation, the broth culture was centrifuged at 1000xg for 10 min. The bacterial cells were washed two times and finally resuspended with a sterile phosphate buffered saline (PBS) – pH 7.2. The obtained suspension was standardized using densitometer (Densimat, bioMerieux) to 0.5 Mc Farland and then diluted 1:1000 to the required cell density of approximately 10<sup>5</sup> colony forming units per milliliter (CFU/ml). The exact initial cell count was determined by spread plate method.

##### Experimental procedure

The antibacterial activity of pure and Fe-modified titanium dioxide substrates were tested as a part of the experimental setup, previously described [28]. The disinfection process was carried out at a volume of 100 ml bacterial suspension with an initial cell density of 10<sup>5</sup> CFU/ml and a catalyst concentration of 1 mg/ml. Each sample was poured in a sterile glass flask of 200 ml. Three flasks were used in the photodisinfection experiment: first flask served as a control of bacteria growth – no catalytic powder or radiation was applied and it was kept in dark; to the second and third flask, 100 mg of synthesized powder was added. The second flask was kept in dark, while the third flask was irradiated with UV light. All samples were conducted in continuous stirring with magnetic stirrers to ensure maximum mixing

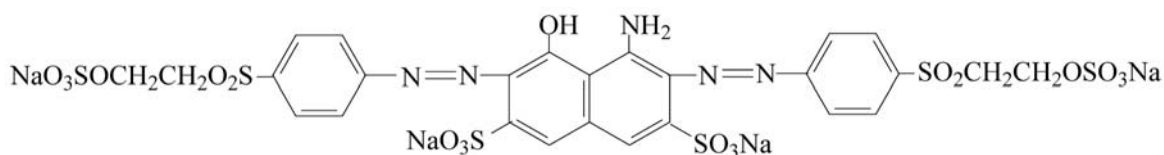


Fig. 2. Molecular structure of Reactive Black 5

of the powder particles. The experiment continued up to 1 hour at room temperature (25 °C).

At regular intervals of time (5 or 10 min) during the experimental period, and after 24 hours in dark, the definite amounts of samples were withdrawn and serial dilutions were prepared. 100 µl of the undiluted samples, and 10<sup>-1</sup> and 10<sup>-2</sup> dilutions were plated on Mueller-Hinton agar, BD Microbiology Systems (Cockeysville, Md). To reduce the detection limit, each undiluted and diluted sample was streaked on 3 agar plates. The number of viable cells in all samples was determined by spread plate method.

Antibacterial effect was evaluated by the decrease in the colony forming units on agar plates and presented as survival curves. The survival curves were constructed by plotting mean survival rate versus time. The removal efficiency, *E*, was calculated as:

$$E = \frac{C_i - C_f}{C_i} \times 100$$

where *C<sub>i</sub>* and *C<sub>f</sub>* are the initial and final CFU/ml, respectively.

## RESULTS AND DISCUSSION

### Characterization of titania samples

XRD measurements were performed to identify the crystalline phases synthesized by the nonhydrolytic sol-gel process at 500 °C calcination temperature. The XRD patterns of the as obtained powders, undoped and iron doped TiO<sub>2</sub> (0.5, 1 and 2 mol% Fe), are shown in Figure 3 a and b, respectively. As is seen in both figures, the three strongest interplanar

distances of anatase (TiO<sub>2</sub>) appear at 3.51; 1.89 and 1.66 Å (JCPDS 78-2486). The anatase structure is preferred over other polymorphs for photocatalytic applications because of its higher electron mobility, low dielectric constant and lower density. All commonly known polymorphs of titania consist of TiO<sub>6</sub> octahedra, which share edges and corners in different manners. The TiO<sub>6</sub> octahedron of anatase is slightly distorted [29]. It has to be noticed that iron was not found in the XRD patterns of the investigated samples due to its very low concentrations. The average crystallite size of as prepared undoped TiO<sub>2</sub> and iron doped TiO<sub>2</sub> (0.5, 1 and 2 mol% Fe) calculated from the broadening of the diffraction line using Sherrer's equation is about 20 and 12–15 nm, respectively. As is seen from the obtained values, the crystallite size of undoped TiO<sub>2</sub> is larger than those of Fe-doped TiO<sub>2</sub>. Obviously, the Fe-doping leads to decrease of the crystallite sizes. Our results are in good accordance to the results obtained by Yang et al. [30]. However, there are previous studies which reported controversial results concerning the Fe<sup>3+</sup> doping effect on the crystallite sizes. For example, Wang et al. [31] claimed that Fe<sup>3+</sup> increase the crystallite sizes. Figure 4 presents the infrared spectra of investigated powder samples in the range 1200–400 cm<sup>-1</sup>. As a more sensitive method, the IR spectroscopy was used to verify the main short range orders of the obtained submicron powders. As is seen from the figure, vibrations of the inorganic building units were recognized only. In the spectrum of all samples (Figure 4) bands in the range 470–420 cm<sup>-1</sup> are observed. It is well known and it was also proved in our previous studies, that bands in the absorption range 700–400 cm<sup>-1</sup> could be related to the vibrations of TiO<sub>6</sub> units [32, 33]. Despite

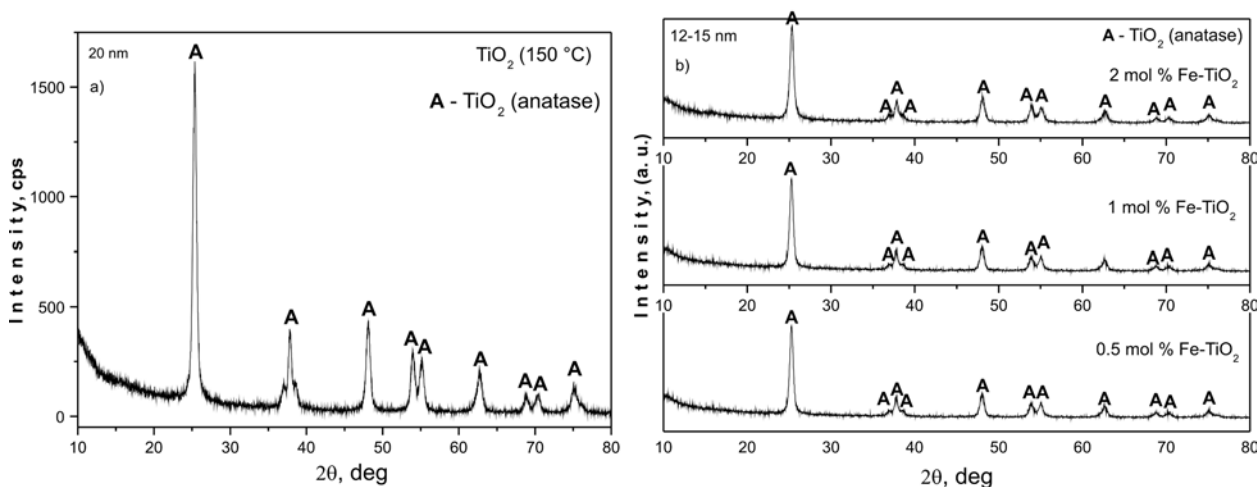


Fig. 3. XRD patterns of undoped (a) and doped with Fe (b) TiO<sub>2</sub>

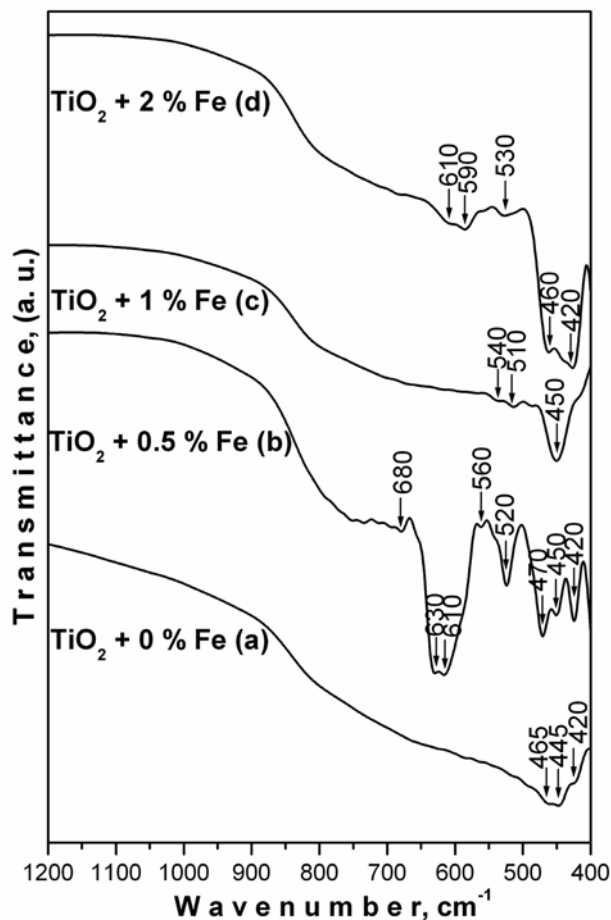


Fig. 4. IR of the investigated samples

the fact that iron was not detected in the XRD patterns, its presence was registered by IR spectroscopy (bands in the range 680–470 cm<sup>-1</sup>). The doping of even small amount of iron (0.5 mol%) led to changes in the IR spectra. The absorption intensity of the new bands changes with the iron content. The observed bands in the range 590–510 cm<sup>-1</sup> could be assigned to the vibrations of FeO<sub>6</sub> structural units, while those above 600 cm<sup>-1</sup> may be related to the vibrations of FeO<sub>4</sub> polyhedra [34].

The ultraviolet-visible (UV-Vis) absorption spectra of different TiO<sub>2</sub> powders are illustrated in Figure 5. As is seen from the figure, the increase in Fe<sup>3+</sup> content increased the absorbance in the UV spectra. The UV-Vis spectra were used to determine the optical band gap ( $E_{opt}$ ) of investigated samples. For undoped TiO<sub>2</sub>  $E_{opt}$  was 2.92 eV, while for the other two samples (0.5 and 2 mol%) it was about 2.95 eV. It is known that the band gap value of Degussa P25 is 3.03 eV [35], while for pure anatase is 3.2 eV [36]. Obviously, the band gap energy values of the synthesized undoped and Fe<sup>3+</sup> doped

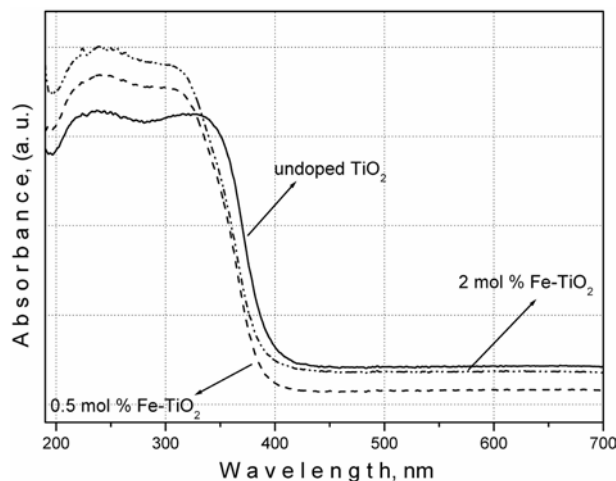


Fig. 5. UV-Vis spectra of undoped and doped with 0.5 and 2 mol% Fe-TiO<sub>2</sub>

TiO<sub>2</sub> samples are lower than those pointed out in the literature [35, 36]. According to Wu et al. [36] the narrowing of the band gap can improve the photocatalytic activity under visible light. This could explain our results for the photocatalytic activity of investigated samples. However, more experiments are needed in order to elucidate this fact.

#### Photocatalytic activity

The water soluble dye RB5 was selected as a model pollutant because it has been extensively used for dyeing cotton fabrics. Reactive Black 5 dye has two reactive vinylsulfonil groups and two azo groups (Figure 2). The dye is not degradable by direct photolysis and by TiO<sub>2</sub> in dark. Decoloration by TiO<sub>2</sub> adsorption under dark conditions did not exceeded 10% for all treatments (data not shown), determining that decoloration was conducted primarily by the photocatalytic process.

The changes in RB5 dye concentration  $C/C_0$  ( $C_0$  initial concentration and  $C$  reaction concentration of the dye) by the synthesized samples with the time of UV and visible radiation are shown in Figures 6 and 7. As can be seen, the iron content is an essential factor to define the photocatalytic activities of the samples. The preparations containing 0.5% Fe showed higher photocatalytic activities than pure TiO<sub>2</sub> either under UV or visible light irradiation. On the other hand, doping with higher concentrations of Fe<sup>3+</sup> ions led to marked decrease in photocatalytic activity.

It is believed that Fe<sup>3+</sup> ions can act as shallow traps in the titania lattice although their role during photooxidation processes remains controversial [37]. Introducing of small amount of dopant ion

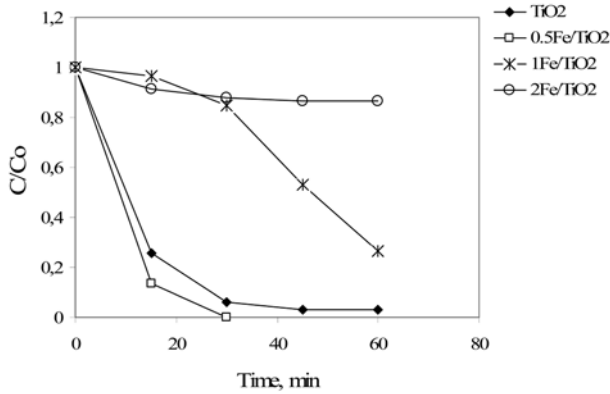


**Fig. 6.** Photocatalytic activity of TiO<sub>2</sub> samples under UV irradiation

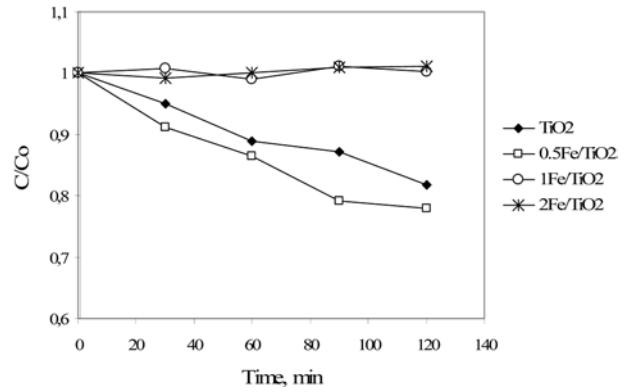


**Fig. 7.** Photocatalytic activity of TiO<sub>2</sub> samples under visible light irradiation

can retard possible electron-hole recombination thus leading to enhanced photoactivity. However, on increasing the dopant content the probability of charge carrier recombination is increased, explained by surplus Fe<sup>3+</sup> ions which can cover the active sites on the surface of TiO<sub>2</sub> particles and as a result the photocatalytic activity decreases [38]. Sources of this controversy could also be due to differences in the preparation methods and doping procedure which can lead to different structural and electronic characteristics of the samples [39, 40]. For a particular synthesis method, optimum dopant concentration directly affect the photocatalytic activity [17, 37]. Such photocatalytic behavior of Fe-doped TiO<sub>2</sub> was observed by us and other researchers. In our study, maximum photoactivity toward RB5 dye was exhibited for the 0.5% Fe sample. The activity of this sample was higher than that of pure TiO<sub>2</sub> (Figures 6 and 7) under both – UV and visible light irradiation.

#### Antibacterial activity

The results from all experiments show that the inactivation of bacteria strongly depends on the presence of UVA light and concentration of the dopant. In the absence of radiation and after 60 min treatment, the number of cells slightly decreased, as follows: from an initial cell count 2.16×10<sup>5</sup> CFU/ml to 1.67×10<sup>5</sup> CFU/ml in contact with pure TiO<sub>2</sub>, and from 2.24×10<sup>5</sup> CFU/ml to 7.40×10<sup>4</sup> CFU/ml with 0.5% Fe-doped TiO<sub>2</sub>. Despite the fact that during dark conditions 0.5% Fe sample had showed better activity and reduced 66.8% of bacterial cells in the first 60 min, in the next 60 min the number of viable cells reached 1.65×10<sup>5</sup> CFU/ml. After 24 hours subsequent dark period, the bacterial growth was the same as at the beginning of the experiment in both

studied powders – pure and 0.5% Fe-doped TiO<sub>2</sub>. It can be concluded, that disinfection with TiO<sub>2</sub> nanosized materials under dark conditions does not proceed. This corresponds to the principle of photocatalytic disinfection activity [11] and is in agreement with other reports [12]. Antibacterial action of the synthesized preparations in the presence of UVA light is illustrated as survival curves in Figure 8. As can be seen, pure TiO<sub>2</sub> exhibited significant photoinduced activity against *E. coli* ATCC 25922: For the initial cell concentration 2.16×10<sup>5</sup> CFU/ml, the removal efficiency in the first 5 and 10 minutes was 49.3% and 98.4%, respectively, and 100% reduction was achieved in 15 min.

Fe-modified titanium dioxide substrates have shown different activities against the tested strain at illumination conditions. It is obvious, that in the presence of UVA light 0.5% Fe-doped TiO<sub>2</sub> ex-

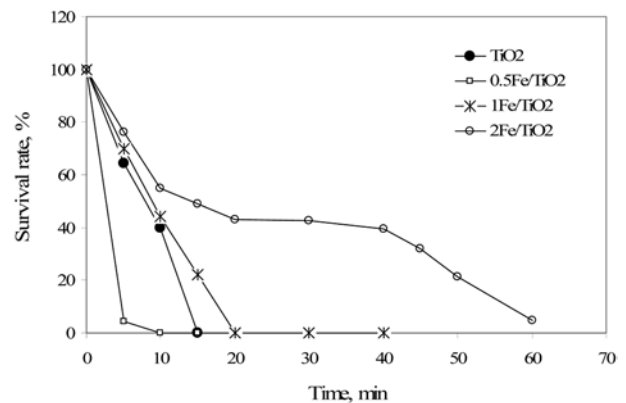


**Fig. 8.** Survival curves of *Escherichia coli* ATCC 25922 in presence of different substances and UVA radiation

hibited strongest antibacterial action – removal efficiency in the first 5 min was 95.7% and complete killing of bacteria was observed in 10 min. Concerning other preparations with higher iron content, the sample 1Fe/TiO<sub>2</sub> showed better antibacterial activity than those of 2Fe/TiO<sub>2</sub> (Figure 8). After 20 min UVA light treatment by 1% Fe-doped TiO<sub>2</sub>, almost all cells were destroyed (99.9%), whereas by using 2% Fe-doped TiO<sub>2</sub> for the same period only half of them were destructed (56.7%) and subsequent 95.3% reduction was achieved after 60 min.

In most studies, TiO<sub>2</sub> photo-inactivation of bacteria has been examined as levels of inactivation without taking into account the levels of repair that may follow [12]. That is why we estimated the post-irradiation effect of all synthesized preparations after 24 h dark period. The subcultures from UVA illuminated TiO<sub>2</sub>, 0.5Fe/TiO<sub>2</sub> and 1Fe/TiO<sub>2</sub> samples did not show any bacterial growth after overnight in the dark. This suggests that photoactivated treatment by these agents induced strong and lethal bacterial damages. In contrast to them, 2% Fe-doped TiO<sub>2</sub> did not show bactericidal effect – *E.coli* re-growth of more than 10<sup>5</sup> CFU/ml was observed after 24 h dark period. Finally, we may assume that some nanosized materials, such as pure TiO<sub>2</sub>, 0.5% and 1% Fe-doped TiO<sub>2</sub> in the presence of UVA light possess bactericidal activity, whereas 2% Fe-doped TiO<sub>2</sub> only inhibits bacterial cells and probably has bacteriostatic effect. Antibacterial activity of Fe-modified titanium dioxide preparations initiated by visible light will be object of further investigations.

## CONCLUSIONS

- Iron-doped titanium dioxide was prepared by a nonhydrolytic sol-gel method using titanium tetrachloride, benzyl alcohol and iron(III) nitrate.
- The optimal iron content for the photocatalytic decomposition of Reactive Black 5 dye under UV-Vis irradiation was found to be 0.5 mol%.
- At higher iron contents (1–2 mol%) the photocatalytic performance under both UV and visible irradiation was worse relative to the undoped TiO<sub>2</sub>.
- In the presence of UV light, both 0.5% and 1% Fe-doped TiO<sub>2</sub> had strong bactericidal activity against *E. coli*, similar to that of the pure TiO<sub>2</sub>. In comparison to them, 2% Fe-doped TiO<sub>2</sub> exhibited only weak bacteriostatic effect.
- The best antibacterial properties under UV illumination were presented by 0.5 mol% Fe-doped TiO<sub>2</sub>, that correlates with highest photocatalytic action of this sample under UVA and Vis irradiation.

**Acknowledgements:** Authors are grateful to the financial support of Medical University-Pleven, Contract No10/2013.

## REFERENCES

1. G. K. Mor, M. A. Carvalho, O. K. Varghese, M. V. Pishko, C. A. Grimes, *J. Mater. Res.*, **19**(2), 628 (2004).
2. O. Carp, C. L. Huisman, A. Reller, *Progr. Solid State Chem.*, **32**, 33 (2004).
3. C. McCullagh, J. M. C. Robertson, D. W. Bahnemann, P. K. J. Robertson, *Res. Chem. Intermed.*, **33**(3–5), 359 (2007).
4. A. Sobczynski, A. Dobosz, *Pol. J. Environ. Studies*, **10**(4), 195 (2001).
5. D. M. Blake, J. Webb, C. Turch, K. Magrini, *Sol. Energy Mater.*, **24**, 584 (1991).
6. T. Tanizaki, Y. Murakami, Y. Hanada, S. Ishikawa, M. Suzuki, R. Shinohara, *J. Health Sci.*, **53**(5), 514 (2007).
7. H. Yang, K. Zhang, R. Shi, X. Li, X. Dong, and Y. Yu, *J. Alloys Compd.*, **413**(1–2), 302 (2006).
8. A. Fujishima, T. N. Rao, D. A. Tryk, *J. Photochem. Photobiol. C*, **1**, 1 (2000).
9. A. R. Khataee, G. Ali Mansoori, Nanostructured Titanium Dioxide Materials: Properties, Preparation and Applications, World Scientific Publishing Co, 2011.
10. S. M. Gupta, M. Tripathi, *Chin. Sci. Bull.*, **56**, 1639 (2011).
11. D. Blake, P. C. Maness, Z. Huang, E. Wolfrum, J. Huang, W. Jacoby, *Sep. Purif. Methods*, **28**(1), 1 (1999).
12. A. G. Rincón, C. Pulgarin, *Appl. Catal. B*, **4**, 99 (2004).
13. D. L. Liao, C. A. Badour, B. Q. Liao, *J. Photochem. Photobiol. A: Chem.*, **194**, 11 (2008).
14. P. Yang, C. Lu, N. Hua, Y. Du, *Mater. Lett.*, **57**(4), 794 (2002).
15. D. Klauson, S. Preis, *Int. J. Photoenergy*, **7**(4), 175 (2005).
16. W. K. Choi, A. Termin, M. R. Hoffmann, *J. Phys. Chem.*, **98**(51), 13669 (1994).
17. A. Kumbhar, G. Chumanov, *J. Nanoparticle Res.*, **7**, 489 (2005).
18. Z. Ambrus, N. Balázs, T. Alapi, G. Wittmann, P. Sipos, A. Dombi, K. Mogyorósi, *Appl. Catal. B: Environ.*, **81**, 27 (2008).
19. W.-C. Hung, S.-H. Fu, J.-J. Tseng, H. Chu, T.-H. Ko, *Chemosphere*, **66**, 2142 (2007).
20. S. Liu, X. Liu, Y. Chen, R. Jiang, *J. Alloys Compd.*, **506**, 877 (2010).
21. E. Piera, M. I. Tejedor-Tejedor, M. E. Zorn, M. A. Anderson, *Appl. Catal. B*, **46**(4), 671 (2003).
22. Z. Li, W. Shen, W. He, X. Zu, *J. Hazard. Mater.*, **155**, 590 (2008).
23. N. D. Abazović, L. Mirengi, I. A. Janković, N. Bibić, D. V. Šojić, B. F. Abramović, M. I. Čomor, *Nanoscale Res. Lett.*, **4**, 518 (2009).

24. A. Di Paola, E. Garcia-Lopez, G. Marci, C. Martin, L. Palmisano, V. Rives, A. M. Venecia, *Appl. Catal. B: Environ.*, **48**, 223 (2004).
25. M. Niederberger, N. Pina, *Metal Oxide Nanoparticles in Organic Solvents*, Springer, 2009.
26. D. P. Debecker, P. H. Mutin, *Chem. Soc. Rev.*, **41**(9), 3624 (2012).
27. M. Niederberger, M. H. Bartl, G. D. Stucky, *J. Am. Chem. Soc.*, **124**, 13642 (2002).
28. A. Stoyanova, M. Sredkova, A. Bachvarova-Nedelcheva, R. Iordanova, Y. Dimitriev, H. Hitkova, Tz. Iliev, *Optoelectron. Advan. Mater.-Rapid Commun.*, **4**(12), 2059 (2010).
29. S. M. Gupta, M. Tripathi. A review of TiO<sub>2</sub> nanoparticles, *Chinese Sci. Bull.*, **56**, 1639 (2011).
30. X. Yang, C. Cao, L. Erickson, K. Hohn, R. Maghirang, K. Klabunde, *Appl. Catal. B: Environ.*, **91**, 657 (2009).
31. Q. Wang, S. Xu, F., Shen, *Appl. Surf. Sci.*, **257**, 7671 (2011).
32. A. N. Murashkevich, A. S. Lavitskaya, T. I. Baranikova, I. M. Zharskii, *J. Appl. Spectr.*, **75**(5), 730 (2008).
33. A. M. Stoyanova, H. Y. Hitkova, A. D. Bachvarova-Nedelcheva, R. S. Iordanova, N. K. Ivanova, M. P. Sredkova, *J. Univ. Chem. Techn. Metall.*, in press.
34. K. Marinaga, Y. Suginoara, Y. Yanagase, *J. Jpn. Inst. Met.*, **40**, 775 (1976).
35. S. Boonyod, W. Sutthisripok, L. Sikong, *Adv. Mater. Res.*, **214**, 197 (2011).
36. H.-C. Wu, S.-H. Li, S.-W. Lin, *Int. J. Photoenergy*, Volume 2012, Article ID 823498.
37. X. Li, P.-L. Yue, C. Kutal, *New J. Chem.*, **27**(8), 1264 (2003).
38. J. Wang, R. Li, L. Zhang, Y. Xie, Z. Jiang, R. Xu, Z. Xing, X. Zhang, *Russ. J. Inorg. Chem.*, **55**(5), 692 (2010).
39. C. Adan, A. Bahamonde, M. Fernandez-Garcia, A. Martinez-Arias, *Appl. Catal. B: Environ.*, **72**, 11 (2007).
40. M. Litter, J. Navio, *J. Photochem. Photobiol. A: Chem.*, **98**(3), 171 (1996).

## ФОТОКАТАЛИТИЧНА И АНТИБАКТЕРИАЛНА АКТИВНОСТ НА ДОТИРАНИ С ЖЕЛЯЗО TiO<sub>2</sub> НАНОЧАСТИЦИ, ПОЛУЧЕНИ ПО НЕХИДРОЛИТИЧЕН ЗОЛ-ГЕЛ МЕТОД

А. М. Стоянова<sup>1\*</sup>, Х. Й. Хиткова<sup>1</sup>, Н. К. Иванова<sup>1</sup>, А. Д. Бъчварова-Неделчева<sup>2</sup>,  
Р. С. Йорданова<sup>2</sup>, М. П. Средкова<sup>1</sup>

<sup>1</sup> Медицински Университет-Плевен, 5800 Плевен, България

<sup>2</sup> Институт по Обща и Неорганична Химия, Българска Академия на Науките,  
1113 София, България

Постъпила февруари, 2013 г.; приета май, 2013 г.

(Резюме)

В настоящата работа е представен синтез на дотиран с желязо TiO<sub>2</sub> синтезиран по нехидролитичен зол-гел метод от титанов тетрафторид, бензилов алкохол и железен(III) нитрат.

Получените образци са охарактеризирани с помощта на РФА, ИЧ и УВ-Вис спектроскопия. Относителният размер на получените Fe-дотирани TiO<sub>2</sub> частици е 12–15 nm.

Фотокаталитичната активност на синтезираните прахове от TiO<sub>2</sub> е изследвана чрез фотодеграцията на органичното багрило Reactive Black 5 при осветяване с УВ и видима светлина.

Антибактериалната активност на чист и Fe-модифициран TiO<sub>2</sub> е изследвана спрямо щам *Escherichia coli* ATCC 25922. Бактериалният растеж беше изпитван в присъствие на съответния синтезиран препарат на тъмно и в присъствие на УВ светлина. Фотодезинфекционната активност е оценена чрез конструиране на „криви на преживяемост“ и определяне на ефективността на отстраняване на бактериалните клетки. За оценка на пост-иррадиационния ефект бактериалната суспензия е тествана отново след 24 ч престой на тъмно. Установено е, че с най-добра фотокаталитична и антибактериална активност е препаратът, съдържащ 0,5 mol% желязо. При по-високо съдържание на желязо (1–2 mol%) фотокаталитичните тестове показаха по-лоши резултати спрямо чистия TiO<sub>2</sub> както в УВ, така и във видимата област.